Dissertationes Forestales 371

Assessing tree growth and competition using laser scanning

Ghasem Ronoud

School of Forest Sciences
Faculty of Science, Forestry and Technology
University of Eastern Finland

Academic dissertation

To be presented, with the permission of the Faculty of Science, Forestry and Technology of the University of Eastern Finland, for public criticism in the auditorium N100 of the University of Eastern Finland, Yliopistokatu 7, Joensuu, on 17 of June 2025, at 12 p.m.

Title of dissertation: Assessing tree growth and competition using laser scanning
Author: Ghasem Ronoud

Dissertationes Forestales 371
https://doi.org/10.14214/df.371

Thesis supervisors:
Professor Mikko Vastaranta
School of Forest Sciences, University of Eastern Finland, Finland

Docent Ninni Saarinen
School of Forest Sciences, University of Eastern Finland, Finland

University Research Fellow, Docent Ville Kankare
Department of Geography and Geology, University of Turku, Finland

Postdoctoral Researcher Tuomas Yrttimaa
School of Forest Sciences, University of Eastern Finland, Finland

Pre-examiners:
Dr. Markus Hollaus
Department of Geodesy and Geoinformation, Vienna University of Technology, Austria

Dr. Lennart Noordermeer
Faculty of Environmental Sciences and Natural Resource Management, Norwegian University of Life Sciences, Norway

Opponent:
Dr. Aarne Hovi
School of Engineering, Aalto University, Espoo, Finland

ISSN 1795-7389 (online)
ISBN 978-951-651-832-2 (pdf)

Publishers:
Finnish Society of Forest Science
Faculty of Agriculture and Forestry of the University of Helsinki
School of Forest Sciences of the University of Eastern Finland

Editorial Office:
Finnish Society of Forest Science
Viikinkaari 6, FI-00790 Helsinki, Finland
http://www.dissertationesforestales.fi

Ronoud, G. (2025) Assessing tree growth and competition using laser scanning. Dissertationes Forestales 371. 39 p. https://doi.org/10.14214/df.371

ABSTRACT

The warming climate, biodiversity loss, and escalating natural disturbances emphasize the need for sustainable forest management, which relies on understanding tree growth and competition. Laser scanning has opened new possibilities for measuring these processes. This thesis aims to develop approaches to evaluate stem and crown growth and competition using laser scanning point clouds, exploring their utility in assessing and quantifying competition dynamics and growth patterns in forest stands.

Study **I** developed approaches for assessing stem and crown competition using terrestrial laser scanning (TLS) point clouds and investigated the effect of different thinning treatments on competition in Scots pine (*Pinus sylvestris* L.)-dominated forests. The results indicated that TLS-derived competition decreased across different thinning methods compared to the control plots for both moderate and intensive thinning. Thinning from below showed the greatest reduction in competition, followed by thinning from above and systematic thinning. Study **I** demonstrates that TLS provides an advanced solution for assessing tree crown characteristics and growing space, highlighting a novel approach to understanding competition between trees.

Study **II** investigated the use of bi-temporal TLS and low-altitude airborne laser scanning (ALS), individually and in combination, to assess the relationship between tree stem volume growth (ΔV) and crown structure, including its change (ΔC), over a 7-year monitoring period. The results showed a strong correlation between ΔV and crown metrics (top height, projection area, and perimeter) for Scots pine. For Norway spruce, ΔV weakly correlated with 3D crown area (CA_{3D}), volume (CV), and its change (ΔCV). Birch ΔV showed weak to moderate correlations with CA_{2D}, crown perimeter, and ΔCV. Random Forest (RF) analyses revealed that changes in crown structure were important for explaining ΔV variations for Norway spruce and birch, while top height (CH_{max}) was the key metric for Scots pine. In conclusion, Study **II** showed that multisensor laser scanning data can serve to evaluate the relationships between ΔV and tree crown structure.

Study **III** examined the utility of TLS and low-altitude ALS data in describing the competitive stress of individual trees using two approaches. The object-based approach quantified competition by identifying and characterizing neighboring trees, while the point cloud-based approach evaluated competition through point cloud structures representing competitive vegetation around a target tree. The results showed that object-based competition indices (CIs) correlated more strongly with *in situ*-based CIs compared to point cloud-based CIs and were more consistent between TLS and ALS. Overall, Study **III** demonstrated that TLS is effective for small-scale competition assessments, while low-altitude ALS has similar potential for describing competition on a large scale.

This thesis demonstrates the capability of the developed laser scanning-based approaches to assess stem and crown growth and competition. It shows how TLS and ALS enhance our understanding of tree growth and their responses to neighboring trees, helping identify processes driving changes in forest dynamics. These findings offer concrete steps toward more precise and efficient forest management, although further refinement of the methodologies is needed to optimize their use across varying forest ecosystems.

Keywords: Boreal forests, Terrestrial laser scanning (TLS), Airborne laser scanning (ALS), Forest monitoring, Point cloud.

ACKNOWLEDGMENTS

This dissertation reflects the growth and knowledge I gained from invaluable interactions with supervisors, peers, colleagues, and friends. I would like to take this opportunity to express my gratitude to the organizations and individuals whose support has been essential to both my academic journey and personal development.

I would like to thank my supervisors, Prof. Mikko Vastaranta, Dr. Ninni Saarinen, Dr. Ville Kankare, and Dr. Tuomas Yrttimaa, who guided me during my doctoral thesis and helped me shape my research ideas. You all gave me the strength to move forward and stay motivated.

I deeply appreciate the valuable collaborations with my co-authors and data providers, as well as the dedicated efforts of those who participated in fieldwork and reference data collection for my studies. Your invaluable contributions have been instrumental in shaping and completing this thesis. In addition, this research was made possible through the financial support of the Research Council of Finland, specifically via the Forest–Human–Machine Interplay Flagship of Science.

I want to thank Dr. Markus Hollaus and Dr. Lennart Noordermeer for pre-examining and improving the present thesis. I am also thankful to Dr. Aarne Hovi for kindly accepting the role of opponent and contributing to the public examination of this work.

I would like to extend my heartfelt gratitude to Maryam Poorazimy for her incredible support, patience, and encouragement throughout this journey. Your unwavering presence made all the difference, and this accomplishment would not have been possible without you.

To my family for their unconditional love and support. You are always a part of my everyday life, no matter the distance.

Thank you all for your contributions to this milestone in my life.

Helsinki, December 2024

Ghasem Ronoud

LIST OF ORIGINAL ARTICLES

This thesis is based on findings presented in the following articles, referred to by the Roman numerals I-III.

I Ronoud, G, Poorazimy, M, Yrttimaa, T, Luoma, V, Huuskonen, S, Hynynen, J, Hyyppä, J, Saarinen, N, Kankare, V, Vastaranta M (2022) Terrestrial laser scanning in assessing the effect of different thinning treatments on the competition of Scots pine (*Pinus sylvestris* L.) forests. Remote Sensing 14(20):5196. https://doi.org/10.3390/rs14205196

II Poorazimy, M, Ronoud, G, Yrttimaa, T, Luoma, V, Bianchi, S, Huuskonen, S, Hyyppä, J, Saarinen, N, Kankare, V, Vastaranta, M (2025) Understanding tree growth dependencies using multisensorial point clouds. European Journal of Forest Research. (Under review)

III Ronoud, G, Poorazimy, M, Yrttimaa, T, Kukko, A, Hyyppä, J, Saarinen, N, Kankare, V, Vastaranta M (2024) Characterizing the competitive stress of individual trees using point clouds. Forest Ecology and Management 57:122305. https://doi.org/10.1016/j.foreco.2024.122305

AUTHOR’S CONTRIBUTIONS

I) Ronoud planned the study together with his supervisors, processed the datasets, conducted all the analyses, and wrote the first draft of the manuscript.

II) Ronoud contributed to the methodology and conceptualization of the study with his colleagues and supervisors and was actively involved in the analysis and manuscript preparation by reviewing and editing.

III) Ronoud planned the study together with his supervisors, processed the datasets, conducted all the analyses, and wrote the first draft of the manuscript.

TABLE OF CONTENTS

ABBREVIATIONS

2D	Two-dimensional
3D	Three-dimensional
ALS	Airborne laser scanning
CA_{2D}	Two-dimensional crown area
CA_{3D}	Three-dimensional crown area
CA_{3D}/CV	Crown surface area-to-volume ratio
CDI	Canopy density index
CHM	Canopy height model
CH_{max}	Crown top height
CH_{min}	Crown base height
CI	Competition index
CI_{CA}	Competition index based on crown projection area
CI_{cs}	Competition index based on crown surface area
CI_{cv}	Competition index based on crown volume
$CI_{Cylinder}$	Competition index based on cylinder method
CI_{dbh}	Competition index based on diameter at breast height
$CI_{dbh\text{-}\mathit{In\ situ}}$	*In situ*-derived competition index based on diameter at breast height
CI_H	Competition index based on tree height
$CI_{H\text{-}\mathit{In\ situ}}$	*In situ*-derived competition index based on height
CI_{MCD}	Competition index based on maximum crown diameter
CIs	Competition indices
CP/CA_{2D}	Crown perimeter-to-projection area ratio
CPI	Competitive pressure index
CS	Crown surface area
CV	Crown volume
dbh	Diameter at breast height
Dg	Mean diameter weighted by basal area
DTM	Digital terrain model
G	Basal area
GNSS	Global Navigation Satellite System
H	Tree height
Hg	Mean height weighted by basal area
IMU	Inertial Measurement Unit
LiDAR	Light detection and ranging
MCD	Maximum crown diameter
N	Stem number per hectare
r	Pearson’s correlation coefficient
RANSAC	Random sample consensus
RF	Random forest
SOCS	Scan Origin Coordinate System
TLS	Terrestrial laser scanning
V	Stem volume
Δ	Growth in tree metrics
ΔC	Growth in crown metrics
ΔCIs	Difference between laser scanning-based CIs and *in situ*-based CIs
ΔV	Growth in stem volume

1 INTRODUCTION

1.1 Background

The increasing impacts of climate change, biodiversity decline, and the rising occurrence of natural disturbances have emphasized the importance of sustainable forest utilization. This necessitates a deep understanding of tree growth and competition for resources. Forests are one of the most valuable terrestrial ecosystems, and studying them is essential to ensure their effective management and high productivity. Trees require key resources for growth, including sunlight, soil nutrients, water, appropriate temperatures, and growing space (Burkhart and Tomé 2012; Tomé and Burkhart 1989). Limited growth resources lead to competition between trees (Burkhart and Tomé 2012). Competition is the main driver of growth in forest stands and for individual trees. It can be quantified using traditional *in situ*-based competition indices (CIs) by considering the dimensions and positions (i.e., diameter at breast height [dbh] and height) of neighboring trees.

Quantifying competition using *in situ*-based CIs is time-consuming and labor-intensive. In addition, the range of suitable tree attributes available for calculating *in situ*-based CIs is quite restricted (Burkhart and Tomé 2012; Tompalski et al. 2016). Crown structure is one of the most critical attributes, but its characteristics are practically impossible to measure accurately (Ma et al. 2018; Weiskittel et al. 2011), requiring destructive sampling in some cases. Therefore, developing alternative approaches to quantifying competition between trees is crucial for enhancing our understanding of tree and forest growth dynamics (Ma et al. 2018; Olivier et al. 2016). The use of laser scanning technology is an effective approach to overcoming these limitations.

Laser scanning has been utilized extensively over the past three decades to collect forest resource information and investigate tree and forest structures by obtaining three-dimensional (3D) information (Fassnacht et al. 2024; Su et al. 2016; Wulder and Franklin 2003). It has also been used to quantify competition between trees in several studies (Metz et al. 2013; Olivier et al. 2016; Pedersen et al. 2012, 2013; Seidel et al. 2015; Yrttimaa et al. 2022a). Nonetheless, quantifying competition through laser scanning is still in its infancy and requires further research and understanding (Ma et al. 2018; Pedersen et al. 2012). On the other hand, laser scanning is anticipated to present alternative solutions for describing the competition between trees by generating highly detailed 3D point clouds. Therefore, accurately quantifying competition using laser scanning point clouds will enhance growth modeling (Bollandsås and Næsset 2009; Twery and Weiskittel 2013). It will also enable forest managers to make more informed and practical decisions regarding activities such as thinning, harvesting, and planning sustainable forest management strategies (Tomé and Burkhart 1989).

1.2 Quantifying competition between trees using *in situ* data

Using *in situ* data in forest stands, competition between trees has traditionally been quantified using two main types of CIs, namely distance-dependent and distance-independent (Pont et al. 2021; Versace et al. 2019). Distance-dependent CIs quantify the competitive stress of trees by considering the distance between a target tree and its neighboring trees, while distance-independent CIs do not rely on the spatial arrangement of individual trees (Burkhart and

Tomé 2012). Both distance-dependent and distance-independent CIs utilize *in situ* measurement information, such as dbh and the height of individual trees, to quantify competition.

Field measurements are needed to describe the competitive stress of trees using *in situ* data and traditional CIs. However, measuring tree attributes, especially for a large number of stands, is time-consuming and labor-intensive. Furthermore, this method is primarily suitable for measuring stem characteristics, such as dbh and tree height, and cannot capture crown structure information, which is essential for accurately quantifying competition among trees. Crown structure plays a significant role in tree interactions and influences overall forest dynamics (Ma et al. 2018). Crown structure refers to the three-dimensional arrangement of foliage and branches within a tree's crown. Key parameters describing crown structure include crown diameter, crown length, crown base height, crown volume, and crown surface area (Zhu et al. 2021). Forest structure, on the other hand, encompasses the spatial organization and vertical layering of trees and vegetation within a stand. It is typically characterized using variables such as tree density, basal area, canopy cover, canopy height, and vertical foliage distribution (Latham et al. 1998). These structural attributes are critical for understanding competition, light availability, and ecosystem functioning (LaRue et al. 2019).

To overcome these limitations, an alternative approach that can accurately and comprehensively capture tree and forest structures is needed. In this regard, laser scanning technology has proven to be a viable approach to the 3D characterization of trees and forests (Tempel et al. 2015; Wulder and Franklin 2003). Laser scanning allows for accurate measurements of tree dimensions, spatial distribution, and crown structures, establishing itself as a promising tool for assessing competition in forest stands (Ma et al. 2018; Olivier et al. 2016).

1.3 Characterizing competition using point clouds

1.3.1 Laser scanning to characterize trees and forests

Laser scanning is an active remote sensing technology that operates based on light detection and ranging (LiDAR) principles, wherein laser light, typically at a specific wavelength, is emitted toward a target and reflected back to the sensor. The sensor records this back-scattered energy and determines the distance to the target using either the phase difference between emitted and received signals (phase-shift approach) or the time it takes for the pulse to travel to the target and back (time-of-flight approach). By repeating this process hundreds of thousands of times per second, laser scanning rapidly reconstructs the 3D structure of objects of interest. This non-destructive technology generates a point cloud—a detailed 3D reconstruction of tree and forest structures—using reflected laser pulses from surfaces such as tree stems and crowns (Tempel et al. 2015; Wulder and Franklin 2003). To ensure accurate georeferencing of the scanned data, the system also incorporates Global Navigation Satellite System (GNSS) and Inertial Measurement Unit (IMU) sensors, which together with the Scan Origin Coordinate System (SOCS), provide the necessary positional and orientation information during data acquisition (Maltamo et al. 2014).

Two important types of laser scanning systems, namely terrestrial laser scanning (TLS) and airborne laser scanning (ALS), have been developed, offering unique potential for studying forest ecosystems (Dassot et al. 2011; Vauhkonen et al. 2014).

TLS is a ground-based LiDAR system important for addressing key ecological questions, enabling us to advance our understanding of fundamental ecological processes (Calders et al. 2020). It is a close-range sensing system that can capture detailed information from tree stems and crown structures (Maas et al. 2008; Muhojoki et al. 2024). TLS point clouds have been successfully applied in various forest inventory measurements, canopy characterization, and aspects of ecology (Dassot et al. 2011). Some of these studies focus on key parameters such as volume (Lefsky and McHale 2008) and biomass (Holopainen et al. 2012; Kaasalainen et al. 2014), wood properties (Pyörälä et al. 2019), and forest inventory (Liang et al. 2016; Newnham et al. 2015).

ALS data is collected from above the canopy using scanners mounted on aerial platforms (e.g., airplanes, helicopters, and drones). These platforms transmit multiple laser pulses from various angles, enabling the acquisition of detailed 3D point clouds of the target. ALS is optimal for studying trees and forests in larger areas to measure canopy height and tree density. It has been used more frequently than TLS for growth and competition studies due to its earlier development. One limitation of the current generation of ALS data is its inability to capture under-canopy details, such as tree stem structure (Terryn et al. 2022).

In general, the differences between TLS and ALS arise from their scanning geometries: TLS favors horizontal forest characterization with high-resolution detail, while ALS provides vertical characterization suitable for large-scale assessments. Thus, they offer complementary approaches to forest measurement.

1.3.2 Utilizing point clouds to characterize competition between trees

In contrast to conventional *in situ*-based methods, point cloud data from TLS and ALS provide more precise measurements of tree space occupancy, allowing for a more accurate estimation of competitive pressure by analyzing the spatial arrangement and proximity of neighboring trees. Point cloud-based approaches, such as the upside-down search cone method, enable the identification of competitive interactions by quantifying the space around each tree, providing a clearer understanding of how competition affects tree growth. These techniques offer an advantage in assessing a large number of forest stands, as traditional methods often lack spatial continuity and are limited by the absence of area-wide data, making it difficult to capture fine-grained competition dynamics.

In recent years, several studies have implemented ALS data to describe tree growth and the competition between trees. For example, Pedersen et al. (2012) quantified individual tree-level competition using ALS data and revealed that these data are preferable to field data. Ma et al. (2018) used bi-temporal ALS data to quantify individual tree growth and competition. Their study showed that ALS is an accurate and robust tool on large scales. Versace et al. (2019) utilized ALS data to predict CIs and concluded that they have a high capacity for quantifying competition at the individual tree level. A few studies have also implemented TLS to describe the competition between trees. For example, Seidel et al. (2015) used TLS point clouds to investigate the effects of competition on tree diameter increment, demonstrating the potential of TLS data. Pitkänen et al. (2022) also showed that TLS is an appropriate technology for quantifying the effects of competition on Scots pine and Norway spruce crown dimensions. Olivier et al. (2016) also used TLS point clouds to examine the effect of competition on sugar maple tree crown growth.

1.4 Thesis objectives

The main objective of this thesis is to develop methodologies for assessing (a) tree growth and (b) the competition between trees using laser scanning data. This is particularly valuable because measuring tree crown structure and dimensions accurately through traditional *in situ*-based methods is challenging and labor-intensive. To accomplish this, the thesis is structured into three interrelated studies that investigate different aspects of competition, growth, and structural characteristics using TLS and ALS point clouds.

The main objective of Study **I** is to develop approaches for assessing crown and stem competition using TLS point clouds and evaluate how different thinning treatments, varying in type (i.e., thinning from below, thinning from above, and systematic thinning) and intensity (i.e., moderate and intensive) affect stem- and crown-based competition between trees. The study aims to answer the following question:

- How do different thinning types and intensities influence the stem and crown competition of Scots pine trees?

Study **II** investigates how bi-temporal TLS and ALS point clouds and their combination can be used to assess the relationship between tree stem volume growth and crown structural changes. In this study, we assume that the combined use of TLS and ALS data will improve tree growth monitoring compared to the use of single-sensor data. The study aims to answer the following question:

- To what extent can a combination of bi-temporal TLS and ALS point clouds reveal the variation in stem volume growth, explained by stem and crown metrics, along with their changes?

Study **III** complements the previous studies by evaluating the capacity of TLS and ALS data to characterize the competitive stress of individual trees. This study addresses how these two data sources can be used to accurately quantify competition through object-based and point cloud-based CIs. The study aims to answer the following question:

- How can the competitive stress of individual trees be described using TLS and ALS data?

Overall, these three studies provide a comprehensive evaluation of tree growth and competition between trees using laser scanning data. Study **I** develops approaches for assessing stem and crown competition using TLS point clouds and examines how thinning treatments with different types and intensities influence stem- and crown-based competition between trees. Study **II** uses bi-temporal TLS and ALS data and their combination to examine the relationship between crown structure changes and stem volume growth. Finally, Study **III** examines the potential of TLS and ALS point clouds in describing the competitive stress of individual trees. The findings from these three studies enhance our understanding of tree dynamics in boreal forests by utilizing different sources of laser scanning 3D point clouds.

2 MATERIALS

2.1 Study sites and field inventory data

Study **I** was carried out in three forest locations: Palomäki (62°3.6′N 24°19.9′E), Pollari (62°4.4′N 24°30.1′E), and Vesijako (61°21.8′N 25°6.3′E) located in the southern boreal forest zone in the municipalities of Mänttä-Vilppula and Padasjoki (Figure 1). The Palomäki study site was established in 2005, and the Pollari and Vesijako study sites were established in 2006 to evaluate the effects of different thinning treatments on Scots pine trees. The Natural Resources Institute Finland (Luke) established and manages all these study sites. The dominant species in these three sites is Scots pine (*Pinus sylvestris* L.), and the stands are considered even-aged, approximately 50 years old. All these forests have relatively flat terrain, and the mean elevation above sea level in Palomäki, Pollari, and Vesijako is 135 m, 155 m, and 120 m, respectively.

A total of 27 rectangular sample plots with varying sizes (1000 m^2 to 1200 m^2) were used to conduct this study (Figure 1). Each of the three study sites had nine sample plots. The thinning experimental design in Study **I** for each study site included three thinning types and two thinning intensities, resulting in six different thinning treatments: (1) moderate thinning from above (four plots), (2) moderate thinning from below (three plots), (3) moderate systematic thinning from above (five plots), (4) intensive thinning from below (three plots), (5) intensive thinning from above (four plots), and (6) intensive systematic thinning from above (five plots). In addition, one un-thinned sample plot (three plots in total without thinning treatment) was established at each study site as a control.

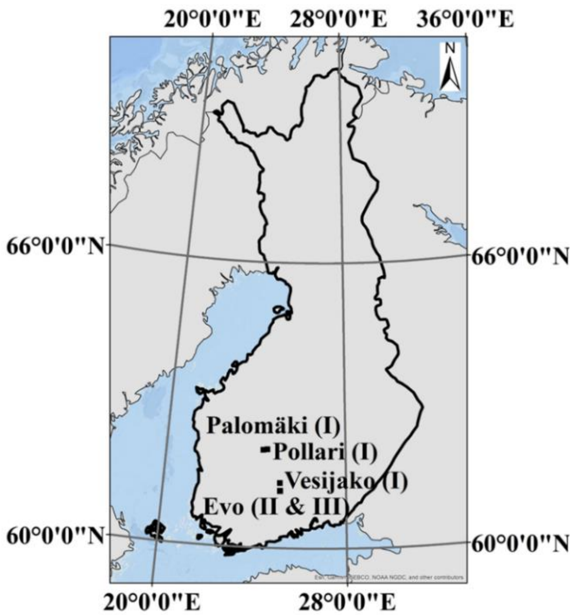

Figure 1. Location of Evo forest (Studies **II** and **III**), along with the Palomäki, Pollari, and Vesijako study sites (Study **I**).

Trees to be removed in each thinning treatment were selected as follows. In thinning from below, co-dominant and suppressed trees were removed, whereas, in thinning from above, mostly dominant trees were considered for removal. In systematic thinning from above, only dominant trees were removed, while small and suppressed trees were left to grow. Moderate thinning resulted in the removal of 32% of the initial basal area, while intensive thinning led to the removal of 66% of the initial basal area. The post-thinning period for evaluating competition response in the remaining trees was 13 years at the Palomäki site and 12 years at the Pollari and Vesijako sites. Table 1 presents a plot-level comparison of different thinning treatment characteristics, including control plots, both before (2005–2006) and after (2005–2006) thinning treatments, as well as after the growth period (2018–2019).

Studies **II** and **III** were conducted in the Evo study site (61°19.6′ N, 25°10.8′ E), located in the southern boreal forest of Finland (Figure 1). Scots pine and Norway spruce (*Picea abies* (L.) H. Karst.) are the two dominant species in this study site. The altitude in the study area ranges from 125 m to 182 m above sea level. The experimental design of Studies **II** and **III** included 22 rectangular sample plots, each measuring 32 m × 32 m, established in 2014 as part of the TLS benchmarking project (Liang et al. 2018). The sample plots were selected to capture a range of stand conditions typical of boreal forests. As a result, they encompass a variety of forest structures, comprising both managed and single-layered forests, as well as unmanaged and multi-layered forests. Field measurements were conducted *in situ* during the summer of 2014. In each sample plot, the dbh, height, and species of all trees with a dbh exceeding 5 cm were measured and recorded. The dbh and height of trees were measured using a caliper and electronic clinometer, respectively. Table 2 summarizes the structural characteristics of the sample plots derived from the *in situ* measurements for the years 2014 (T1) and 2021 (T2).

Table 1. Mean plot-level characteristics before thinning treatments (2005–2006), following thinning treatments (2005–2006), and after the growth period (2018–2019). G = basal area (m2/ha), N = stem number per hectare, V = volume (m3/ha), Dg = mean diameter weighted by basal area (cm), Hg = mean height weighted by basal area (m).

		Before Thinning (2005–2006)		
	No Treatment	Thinning from Below (Moderate/Intensive)	Thinning from Above (Moderate/Intensive)	Systematic Thinning (Moderate/Intensive)
G (m^2/ha)	27.6	26.9/26.9	27.8/24.7	25.4/26.0
N/ha	1336	1285/1260	1417/1201	1256/1218
V (m^3/ha)	224.4	215.4/216.6	216.9/191.0	199.7/210.6
D_g (cm)	17.8	17.5/18.0	17.3/17.6	17.5/18.0
H_g (m)	16.1	16.1/16.3	15.9/15.6	15.9/16.2
		After Thinning (2005–2006)		
	No Treatment	Thinning from Below (Moderate/Intensive)	Thinning from Above (Moderate/Intensive)	Systematic Thinning (Moderate/Intensive)
G (m^2/ha)	27.6	18.3/8.9	18.5/9.1	18.2/8.7
N/ha	1336	719/292	955/479	988/522
V (m^3/ha)	224.4	148.8/72.9	144.0/69.1	141.3/67.3
D_g (cm)	17.8	18.7/20.4	16.9/16.5	16.5/15.7
H_g (m)	16.1	16.5/16.9	15.7/15.3	15.6/15.5
		After the Growth Period (2018–2019)		
	No Treatment	Thinning from Below (Moderate/Intensive)	Thinning from Above (Moderate/Intensive)	Systematic Thinning (Moderate/Intensive)
G (m^2/ha)	37.1	28.4/15.9	28.3/16.1	27.6/15.9
N/ha	1249	705/286	915/446	937/466
V (m^3/ha)	380.3	291.8/160.8	282.3/150.5	267.9/150.4
D_g (cm)	21.2	23.5/27.5	21.2/22.3	20.7/22.2
H_g (m)	21.3	21.7/21.6	21.0/19.5	20.3/20.0

Table 2. Summary statistics of the structural characteristics of the plots based on *in situ* measurements for Studies **II** and **III**, including the minimum (Min), mean, maximum (Max), and standard deviation (Std.) of the number of trees per hectare (N), mean volume (V), mean diameter weighted by basal area (Dg), and mean height weighted by basal area (Hg).

Study	**Year**	**Attribute**	**N (n/ha)**	**V (m^3/ha)**	**Dg (cm)**	**Hg (m)**
II & III	2014	Min	430	110.64	13.91	13.03
		Mean	1238	297.24	25.93	21.01
		Max	3008	482.33	41.58	27.04
		Std.	731	115.21	9.10	4.14
II	2021	Min	430	143.89	16.08	14.80
		Mean	1197	356.42	27.91	22.50
		Max	2568	537.24	42.41	28.14
		Std.	674	117.14	8.79	3.80

2.2 Laser scanning data acquisition

2.2.1 Laser scanning data in Study I

TLS data in Study **I** were acquired using a Trimble TX5 3D (Trimble Inc., Sunnyvale, California, USA) phase-shift laser scanner between September and October 2018 (Table 3). This scanner operates at a wavelength of 905 nm and can measure up to 976,000 points per second, with a beam divergence of 0.19 mrad. Each scan covers 360 degrees horizontally and 300 degrees vertically. A multi-scan approach was used for TLS data acquisition to ensure that the point clouds characterized all trees. The scanner was positioned at eight distinct locations evenly distributed around each sample plot to collect point clouds. Two of these locations (referred to as central scans) were near the center of the plot, a few meters apart, while the remaining six (referred to as auxiliary scans) were evenly distributed around the perimeter of the plot, favoring positions near the plot borders. Point clouds from the various scan locations were registered using artificial reference targets—white spheres with a diameter of 198 mm—mounted on tripods and distributed around the sample plot. The maximum horizontal distance between the scanner and a tree was about 7 m. At this distance, the scanning parameters used produced a point spacing of 2.7 mm in the point cloud from a single scan. Depending on the structure of the sample plot, the resulting overall point density ranged from 52,000 to 91,000 pts/m^2 (Table 3).

2.2.2 Laser scanning data in Study II

TLS data in Study **II** were acquired in 2014 (T1) and 2021 (T2) across the studied sample plots (Table 3). The T1-TLS data were collected by a Leica HDS6100 (Leica Geosystems, St. Gallen, Switzerland) phase-shift scanner in April–May 2014. The scanner operated at a wavelength of 690 nm and could capture high-density point clouds with a scanning rate of 508,000 points per second. The resulting point cloud from a single scan exhibited hemispherical (360° horizontal × 310° vertical) coverage, providing detailed 3D information in both the horizontal and vertical directions, with an angular resolution of 0.018° (Table 3). To obtain a comprehensive point cloud for each sample plot, five individual scans were performed from different locations. The scan configuration included a central scan positioned at the plot center, along with four auxiliary scans strategically placed in the quadrant directions (northeast, southeast, southwest, and northwest), each approximately 11 m from the center. Different individual scans were co-registered using artificial reference targets as control points in Z + F LaserControl (Zoller + Fröhlich GmbH, Wangen im Allgäu, Germany) point cloud processing software to generate a unified point cloud.

A Leica RTC360 3D time-of-flight scanner (Leica Geosystems, St. Gallen, Switzerland) acquired the T2-TLS data in April–May 2021 (Table 3). The scan setup was different from that for T1-TLS, and in addition to the central scan, eight auxiliary scans were performed approximately at the plot borders (angular resolution of 0.009°); see Table 3. The same co-registration process with a similar level of accuracy was applied to the T2-TLS point clouds using Leica Cyclone 3D point cloud processing software (Leica Geosystems AG, Heerbrugg, Switzerland). The existing tree maps were updated to include trees that had reached the measurement threshold (dbh of at least 5 cm). Additionally, trees that had been harvested or had fallen during the monitoring period were removed from the tree maps.

The low-altitude ALS data in Study **II** were also acquired in 2014 (T1) and 2021 (T2) across the study area (Table 3). The T1-ALS data in Study **II** were acquired using a Riegl

VQ-480-U scanner (RIEGL Laser Measurement Systems GmbH, Horn, Austria) from a helicopter flying at an altitude of 75 m. A constant flight speed of 50 km/h was maintained. The ground footprint size was about 2.3 cm. In addition, on-ground pulse spacing along the scan line and between scan lines was approximately 4.7 cm and 9.3 cm, respectively. To ensure data quality, erroneous points were manually removed. This involved carefully identifying and eliminating points that originated from incorrect returns, such as isolated points in the sky or below ground level. The ALS point clouds were captured with a high level of detail and precision, resulting in a point density of approximately 450 pts/m^2.

The T2-ALS data were acquired using a multi-sensorial system carried by a helicopter with a target flying speed of 50 km/h in June 2021. The implemented scanners included three Riegl laser scanners: the VUX-1HA, the MiniVUX-3UAV, and the VQ-840-G (RIEGL Laser Measurement Systems GmbH, Horn, Austria). The flight height was approximately 80 m above ground level, resulting in a point density of 3200 pts/m^2 and a point spacing of 2.0 cm on the ground (Table 3).

2.2.3 Laser scanning data in Study III

The data used in Study **III** were the same T1-TLS (2014) and T1-ALS (2014) data used in Study **II** (Table 3).

Table 3. Acquisition setup of laser scanning datasets, including terrestrial laser scanning (TLS) and airborne laser scanning (ALS), performed in 2014, 2018, and 2021.

Specification	**2014 (Studies II & III)**		**2018 (Study I)**	**2021 (Study II)**	
	TLS	**ALS**	**TLS**	**TLS**	**ALS**
Sensor	Leica HDS6100	Riegl VQ 480-U	Trimble TX5 3D	Leica RTC360 3D	Riegl VUX-1HA / MiniVUX-3UAV / VQ-840-G
Wavelength	690 nm	1550 nm	905 nm	1550 nm	1550/905/532 nm
Beam divergence	0.22 mrad	0.3 mrad	0.19 mrad	0.16 mrad	0.5/0.5 × 1.6/1 mrad
Field of view	310° vertically and 360° horizontally	60°	300° vertically and 360° horizontally	300° vertically and 360° horizontally	360°/120°/40°
Pulse repetition rate	508 kHz	550 kHz	976 kHz	2000 kHz	1017, 300, 200 kHz
Platform	Tripod	Low-altitude helicopter	Tripod	Tripod	Low-altitude helicopter

2.3 Deriving individual tree structural metrics from point clouds

In this section, the methods for deriving individual tree structural metrics from TLS and ALS point clouds from the three studies were integrated to characterize tree structure. The first step in the analysis involved classifying point clouds into ground and non-ground points. TLS and ALS data were processed using LAStools software (rapidlasso GmbH, Gilching, Germany). Using the lidR package, triangulated irregular network models were created to generate TLS- and ALS-based digital terrain models (DTMs) with a resolution of 0.5 m (Roussel and Auty 2018). Subsequently, the TLS and ALS point clouds were normalized using their respective DTMs, and only the points representing vegetation were selected for further analysis. TLS- and ALS-derived canopy height models (CHMs) were created from the height-normalized TLS and ALS point clouds using the pit-free algorithm (Khosravipour et al. 2016) in LAStools. This algorithm combines a standard CHM with partial surface models generated from the highest return points near pits. This study produced partial CHMs using height thresholds of 2, 5, 10, 15, 20, 25, 30, 35, and 40 m. The normalized point clouds were thinned to half the pixel size for this process. A near-ground surface model was created to address potential holes by excluding points above 10 cm (Isenburg 2019). Finally, the CHM and partial surface models were combined into a single CHM with a 0.5 m pixel size, using the highest values from all the CHM or partial surface models. In Study I, the resolution of the CHM obtained was 0.2 m.

To analyze individual trees, the local maxima filter algorithm was applied to the final CHM of the sample plot using the lidR package in R. A fixed window size of 3 × 3 pixels, determined through experimental testing, was used to identify the treetops. An exception to this approach can be found in Study I, where a variable window size was used for segmenting trees from TLS data. In the next step, the final CHM was segmented into individual tree crowns (i.e., 2D crown segments) utilizing a marker-controlled watershed segmentation algorithm (Meyer and Beucher 1990). The identified tree crown segments were used to clip out the points corresponding to each tree using a point-in-polygon approach applied to the XY plane. Moreover, TLS-derived individual tree point clouds were classified per the methodology developed by Yrttimaa et al. (2020). It is based on separating points originating from the stem and crown. It applies surface normal filtering and random sample consensus (RANSAC)-cylinder filtering across height intervals to identify point cloud clusters that formed smooth, vertical, and cylindrical structures representing the tree stem. An alpha shape was then generated to enclose these points, while any points outside the alpha shape were assumed to represent the tree crown. In the ALS point clouds, points delineated by individual trees were classified as crown points if they fell outside the alpha shape but remained within the 2D crown segment. Ultimately, individual tree locations were identified from the TLS point clouds as the center points (XY coordinates) of the RANSAC cylinders fitted to the stem points at breast height. For the ALS point clouds, the tree location was derived as the mean XY coordinates of all points within each 2D crown segment.

Table 4 presents the computed attributes used to characterize individual trees based on the TLS and ALS point clouds. Tree height was determined using the highest point return within each tree segment. Additionally, to extract the crown structure and relevant geometric features, a 2D convex hull was employed to enclose the crown points from both TLS and ALS data using the rLiDAR package. This approach allowed for the characterization of crown morphology using two key attributes: the 2D crown area (CA_{2D}) and the maximum crown diameter (MCD); see Table 4.

The dbh of individual trees was either directly measured (TLS) or predicted based on tree height (ALS). In the case of TLS, the dbh was calculated by fitting RANSAC cylinders to stem points collected from various heights around breast height (specifically at height intervals of 1.25–1.30 m and 1.30–1.35 m). The average of these diameter measurements from different heights was then used as the dbh estimate (Table 4). For trees where the dbh measurement was either unreasonable (i.e., not falling within the range of approximately 5 cm to 65 cm) or could not be obtained, the dbh was estimated based on tree height using allometric models (Kalliovirta and Tokola 2005). This approach was necessary due to the limitations in characterizing all trees through TLS measurement in this study. For instance, some trees were not fully scanned from all perspectives, resulting in incomplete point cloud representations, which could lead to an overestimation of dbh when derived from point cloud measurements. Similarly, for ALS data, the dbh was estimated using the same allometric equation based on tree height (Kalliovirta and Tokola 2005).

Table 4. Description of metrics characterizing the stem and crown derived from terrestrial laser scanning (TLS), airborne laser scanning (ALS), and a combination of TLS and ALS. In Study **II**, metrics were extracted at two time points in 2014 (T1) and 2021 (T2), while in Study **III**, only T1 (2014) was used. In addition, the change in these metrics over the monitoring period of Study **II** was calculated by subtracting T1 measures from the respective T2 measures (Δ = T2 − T1). dbh: diameter at breast height, H: tree height, MCD: maximum crown diameter, CA_{2D}: crown area 2D, CA_{3D}: crown area 3D, CV: crown volume, CS: crown surface area, V: stem volume, CP: crown perimeter, CP/CA_{2D}: crown perimeter-to-projection area ratio, CA_{3D}/CV: crown surface area-to-volume ratio, CH_{min}: crown base height, CH_{max} (m): crown top height.

Study	Characteristic (Unit)	Description/Calculation
I, III	dbh (cm)	Diameter at breast height (1.30 m) of the individual trees obtained by fitting a RANSAC cylinder in TLS/predicted using allometry (Kalliovirta and Tokola 2005) with tree height for ALS.
I, III	H (m)	Maximum height (Z value) of individual tree point clouds for TLS and/or ALS.
I, III	MCD (m)	Maximum crown diameter based on the 2D convex hull for TLS and/or ALS.
I, II, III	CA_{2D} (m^2)	Area of the crown 2D convex hull projected onto an XY plane for TLS and/or ALS.
II	CA_{3D} (m^3)	Area of a 3D convex hull enveloping crown points.
I, **II**	CV (m^3)	Volume of the 3D convex hull enveloping crown points calculated as the sum of the volumes of 0.1 m voxels occupied by crown points.
I	CS (m^2)	Surface area enveloping crown points based on the 3D convex hull.
II	V (dm^3)	Calculated by considering the stem as a sequence of vertical cylinders.
II	CP (m)	Perimeter of a 2D convex hull enveloping crown points.
II	CP/CA_{2D} (m/m^2)	Ratio of CP to $CA_{2D.}$
II	CA_{3D}/CV (m^2/m^3)	Ratio of CA_{3D} to CV.
II	CH_{min} (m)	Height at which the 3D convex hull enveloping crown points reaches its lowest points.
II	CH_{max} (m)	Highest point within the crown segment; represents tree height.

2.4 Describing the competitive stress of individual trees using laser scanning data

2.4.1 Object-based approach

In Studies **I** and **III**, a distance-dependent object-based approach was used to quantify the competitive stress of each target tree within the plot. In this approach, the size and locations of the target tree and its neighbors are considered. To find the neighboring trees of each target tree, a fixed 8 m distance search zone was defined, as proposed by previous studies (Pedersen et al. 2012; Pont et al. 2021; Zhou et al. 2022). In Study **I**, six different stem- and crown-based CIs were computed for each target tree as a sum of inverse distances to the neighboring trees weighted by the dbh (CI_{dbh}), tree height (CI_H), tree maximum crown diameter (CI_{MCD}), crown projection area (CI_{CA}), crown volume (CI_{cv}), and crown surface area (CI_{cs}) following the Hegyi equation (Hegyi 1974); see Equation (1). In Study **III**, only the first three CIs (CI_{dbh}, CI_H, and CI_{MCD}) were utilized.

$$\mathrm{CI} = \sum_{i=1}^{n} (\mathrm{X_i}/(\mathrm{X} \times \mathrm{dist_i})) \tag{1}$$

where CI indicates the competition index for a given individual target tree; *n* represents the total number of neighboring trees located within an 8 m search zone; $\mathrm{X_i}$ represents the dbh, height, maximum crown diameter (MCD), crown projection area (CA), crown volume (CV), and crown surface area (CS) of the i^{th} neighboring tree; *X* refers to the corresponding attributes of the target tree; and $\mathrm{dist_i}$ indicates the horizontal distance between the target tree and the *i-th* neighboring tree.

To avoid edge effects, trees located within 8 m of the plot border were excluded from the computation of CIs. However, in Study **I**, a larger buffer of 11 m was applied for this exclusion. This also ensured that the TLS scan setup provided a complete, multi-viewpoint reconstruction of the trees (Yrttimaa et al. 2019). In addition, non-normalized tree height was restored via DTMs to consider the effect of topography on CIs based on tree height.

2.4.2 Point cloud-based approach

In Study **III**, a point cloud-based approach was used to quantify competition as an alternative to the object-based approach. In this approach, the competitive stress of the target trees was quantified based on canopy occupancy within the crown neighborhood and the geometric relationships between the target tree and its neighbors. Here, two methods were used to identify the vegetative structures of neighboring trees that contribute to competition. This included (1) a search-cone method that determined the competitive space as an upside-down cone with an opening angle of 60° positioned at a 60% relative tree height (Seidel et al. 2015)and (2) a search-cylinder method that determined the competitive space as a vertical cylinder expanding around the target tree with a radius of 4 m. To account for the impact of topography on the quantified CIs, non-normalized TLS and ALS point clouds were utilized for this point cloud-based approach. Notably, CIs were not calculated for trees located within 8 m of the plot boundary to minimize edge effects, consistent with the object-based approach.

In the search-cone method, the search cone was first established based on tree dimensions. The cone was set to extend from the 60% relative height to the top of the tree. The small-end diameter of the search cone at the 60% relative tree height was defined as the corresponding crown diameter. This was derived by enveloping a horizontal cross-section of the non-stem points of each target tree with a 2D convex hull. After establishing the search cone, points that were located within the search cone but outside the 3D convex hull of the target tree crown were delineated utilizing the non-normalized point clouds from the sample plots. These points were classified as neighboring points and considered to represent competing vegetative structures. These points were further voxelized into a 0.1 m × 0.1 m × 0.1 m grid, with each voxel indicating 0.001 m^3 of vegetation-occupied space around the crown of the target tree.

Using three elements, namely neighboring point clouds, the search cone's geometry, and the target tree's crown characteristics, the canopy density index (CDI) and competitive pressure index (CPI) were calculated. The initial step consisted of a volumetric analysis to assess the presence of vegetative structures within the competitive space. The volume of space occupied by neighboring point clouds (CV) was calculated by multiplying the number of neighboring points (with $Z \leq$ the height of the target tree) by their representative volume of 0.001 m^3. The relative volume of the space occupied by neighboring trees (i.e., CDI) was defined as the ratio between the CV and the volume of the search cone whose top surface was constrained to the height corresponding to the tree height (V_{cone}), excluding the volume of the target tree's crown (V_{crown}). V_{cone} was calculated using the geometric equation for the volume of a truncated cone. A 3D version of the CPI was utilized to consider the distance of the neighboring trees. Hence, the CPI was computed as a mean inverse Euclidean distance between the neighboring points and the surface of the 3D convex hull of the target tree crown (Figure 2).

As mentioned before, the search cylinder method was also used to quantify the competitive stress of target trees. Calculating the filling of the cylindrical space was significantly more straightforward with this method than with the conical filling method, as it did not require conversion into spherical coordinates (Seidel et al. 2015). Consequently, the number of 1 dm^3 voxels with centers located within a 4 m radius of the search cylinder were counted, which allowed for determining the corresponding vegetation-occupied volume, referred to as $CI_{Cylinder}$ (Figure 2). In line with Seidel et al. (2015), the 4 m radius search cylinder was utilized due to its better performance compared to larger or smaller search cylinders, according to our initial experiments.

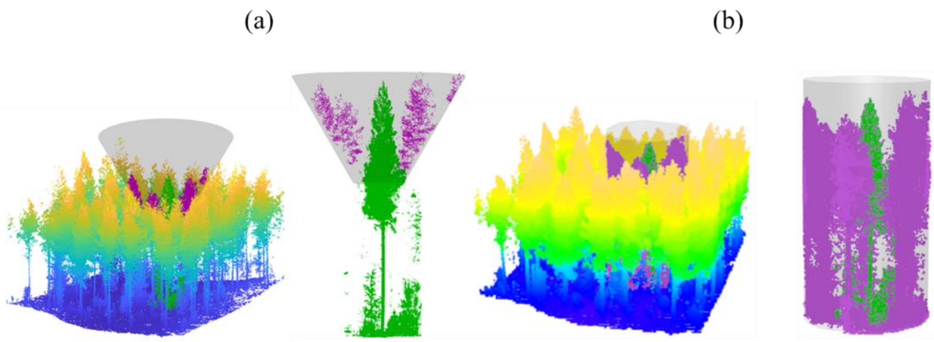

Figure 2. Depiction of (a) the search-cone method and (b) the cylinder-based method to describe the competitive stress of target trees. The target tree is highlighted in green, while the point cloud structures identified as competing neighbors are represented in purple.

2.5 Quantifying the competitive stress of individual trees using *in situ* data

In Study **III**, CIs derived from *in situ* data were used to evaluate the reliability of the competition between trees quantified from laser scanning techniques. In the same way as the object-based CIs (Section 2.4.1), the Hegyi equation was calculated using dbh ($CI_{dbh\text{-}In\ situ}$) and height ($CI_{H\text{-}In\ situ}$) to compute the magnitude of competition affecting each *in situ* target tree. Like before, the computed *in situ*-based CIs for trees closer than 8 m from the plot border were excluded to mitigate the edge effect. It is important to note that $CI_{H\text{-}In\ situ}$ was solely utilized to evaluate the accuracy of the predicted CI_H, while the other CIs were compared against $CI_{dbh\text{-}In\ situ}$. In addition, based on findings from previous studies (Contreras et al. 2011; Pedersen et al. 2013; Seidel et al. 2015), relative basal area increment was used to evaluate the reliability of CIs. Hence, in Study **III**, our predicted laser scanning-based CIs were assessed against relative basal area increment, calculated by subtracting the *in situ* basal area in 2014 from the corresponding measure in 2021 and dividing the result by the initial basal area in 2014.

2.6 Tree-to-tree matching

A tree-to-tree matching process was used to link field-measured trees with point cloud-derived trees. Hence, the geospatial locations of the trees were initially used to identify potential counterpart candidates within a defined search range. If multiple candidates were found within the search range, tree characteristic similarity was used as the criterion to determine the correct match. Specifically, in Studies **I** (Table 5) and **III** (Table 7), a search range maximum distance of 2 m was considered. If multiple detected or *in situ* trees fell within this search radius, correspondences were established based on the similarity of their heights. This matching procedure in Study **III**, along with the applied constraints, resulted in the inclusion of a total of 225 TLS trees and 213 ALS trees in the analysis. In Study **III**, the same approach was used to match TLS and ALS trees, allowing the evaluation of the consistency of the CIs derived from both methods. This process resulted in the inclusion of 126 trees in both datasets. In Study **I**, 2076 TLS-derived trees were matched with field-measured trees and used for further analysis. In Study **II**, species information for each extracted tree was determined by identifying the corresponding field-measured tree within a 1.5 m search range around each T1-TLS-measured tree. A similar approach was also used to link T1-TLS measurements with T2-TLS measurements. In both scenarios, if multiple candidates were identified within the search range, tree metrics similarity was used to validate matches, both between field measurements and T1-TLS data and between T1-TLS and T2-TLS measurements. To focus the analysis on trees with adequate point cloud reconstruction at both T1 and T2, the following thresholds for acceptable variability in tree metrics between the subsequent measurements were applied: difference in the field-measured and TLS-derived dbh < 3 cm, difference in TLS-derived diameter at 6 m height < 4 cm, difference in TLS-derived crown volume < 70%, and difference in TLS-derived tree height < 6 m. These thresholds were set based on prior experience with the accuracy and variability of TLS-based tree characterization in the sample plots. The matched trees were categorized by species: Scots pine, Norway spruce, and birch. Summary statistics for the matched trees from the field plots are shown in Table 6.

Table 5. Summary statistics of sample trees in each treatment measured by TLS data in Study **I**.

Attribute	Statistic	No Treatment (*n* = 129)	Thinning from Below		Thinning from Above		Systematic Thinning	
			Moderate (*n* = 76)	Intensive (*n* = 34)	Moderate (*n* = 141)	Intensive (*n* = 62)	Moderate (*n* = 183)	Intensive (*n* = 95)
DBH (cm)	Min	9.75	14.25	17.9	11	14.3	9	11.75
	Mean	16.56	21.77	26.19	19.05	21.87	19.03	21.1
	Max	34.4	31.35	34.65	32.25	28.35	28.8	29.1
	Std.	4.76	3.81	4.04	4.15	2.96	3.74	3.96
Height (m)	Min	14.94	16.98	18.2	16.7	14.9	13.7	13.9
	Mean	20.76	21.13	21.18	20.38	19.28	19.7	19.14
	Max	30.3	25.2	24.8	24.7	22.7	24.9	23.3
	Std.	3.06	2.24	1.66	1.47	1.49	1.85	2.24
Volume (m^3)	Min	0.06	0.13	0.23	0.08	0.12	0.04	0.07
	Mean	0.33	0.39	0.56	0.3	0.36	0.29	0.34
	Max	1.27	0.89	1.03	0.92	0.66	0.73	0.72
	Std.	0.2	0.16	0.19	0.14	0.11	0.12	0.14

Table 6. Summary statistics of the matched trees measured in the field plots by tree species in the years 2014 (T1) and 2021 (T2) for Study **II**. The minimum (Min), maximum (Max), mean, and standard deviation (Std.) of the diameter at breast height (dbh), volume, and height have been reported.

Attributes/ Species Group		Scots Pine (*n* = 219)		Norway Spruce (*n* = 112)		Birch (*n* = 77)	
		2014	2021	2014	2021	2014	2021
Dbh (cm)	Min	5.45	5.20	6.35	6.20	6.50	6.45
	Max	57.10	58.60	50.70	54.00	29.75	32.50
	Mean	19.10	20.76	21.54	23.04	16.60	18.10
	Std.	7.77	8.36	10.02	10.43	5.63	6.04
Volume (m^3)	Min	0.01	0.01	0.01	0.01	0.01	0.01
	Max	3.34	3.87	2.78	3.38	0.77	1.02
	Mean	0.31	0.40	0.52	0.62	0.24	0.31
	Std.	0.37	0.44	0.51	0.59	0.20	0.24
Height (m)	Min	5.80	6.00	5.30	5.40	7.60	7.10
	Max	34.30	36.00	34.40	37.40	29.70	29.50
	Mean	16.75	18.75	19.74	21.23	19.18	20.76
	Std.	4.65	5.09	7.49	7.70	4.66	4.81

Table 7. Minimum (Min), mean, maximum (Max), and standard deviation (Std.) values of structural attributes and competition indices (CIs) for the matched trees of terrestrial laser scanning (TLS) and airborne laser scanning (ALS), along with their *in situ* correspondence for Study **III**. dbh, H, and MCD indicate tree diameter at breast height, height, and maximum crown diameter, respectively. CI_{dbh}, CI_{H}, and CI_{MCD} are the object-based CIs based on dbh, H, and MCD, respectively. The canopy density index (CDI), competitive pressure index (CPI), and $CI_{Cylinder}$ (i.e., vegetation-occupied volume) are point cloud-based CIs. From the TLS point clouds, 225 trees could be identified and matched with *in situ* trees, while the corresponding number for the ALS point clouds was 213. This accounts for the small differences in the characteristics of the *in situ* trees between the TLS and ALS datasets.

Attribute/Competition index (CI)	Dataset	Min	Mean	Max	Std.
dbh (cm)	*In situ*	5.25	20.03	38.80	7.17
	TLS	8.25	21.61	36.24	5.95
	In situ	5.25	20.32	38.80	6.76
	ALS	13.32	24.27	35.04	4.97
H (m)	*In situ*	10.40	20.50	30.20	4.62
	TLS	12.57	20.95	29.45	3.94
	In situ	10.50	20.92	30.20	4.38
	ALS	11.58	21.03	30.32	4.29
MCD (m)	TLS	2.92	5.21	7.72	6.89
	ALS	2.31	5.21	8.53	1.21
CI_{dbh}	*In situ*	0.63	1.84	7.95	1.06
	TLS	0.95	2.41	4.60	0.77
	In situ	0.63	1.70	2.93	0.51
	ALS	0.63	1.95	3.56	0.73
CI_{H}	*In situ*	0.83	1.82	2.77	0.45
	TLS	1.27	2.39	3.56	0.55
	In situ	0.83	1.82	2.77	0.45
	ALS	0.52	1.93	3.47	0.71
CI_{MCD}	TLS	0.74	2.37	4.16	0.77
	ALS	0.34	2	4.03	0.74
CDI	TLS	0.0005	0.03	0.08	0.02
	ALS	0	0.006	0.015	0.004
CPI	TLS	0.5	89.51	242.82	57.68
	ALS	0	16.10	54.58	11.99
$CI_{Cylinder}$	TLS	6322	64949	124297	27151.59
	ALS	0	4935	11352	2872

2.7 Assessments of growth and competition

In Study **I**, a mixed-effects model was applied to assess whether CIs varied across different thinning treatments, as it is suitable for analyzing multiple observations that are often correlated within independent sampling units (Mehtätalo and Lappi 2020). Given that different thinning treatments were applied across multiple plots at three study sites, a nested two-level linear mixed-effects model was used, fitted with Restricted Maximum Likelihood, as implemented in the nlme package in R (Pinheiro et al. 2014); see Equation (2). Tukey's honest significance test was utilized to identify statistically significant differences in CIs resulting from the different thinning treatments.

$$y_{ij} = \beta_1 No\ treatment_1 + \beta_2 Moderate\ below_i + \beta_3 Intensive\ below_i + \beta_4 Moderate\ above_i + \beta_5 Intensive\ above_i + \beta_6 Moderate\ systematic_i + \beta_7 Intensive\ systematic_i + \alpha_i + c_{ij} + \in_{ij} \tag{2}$$

where y_{ij} is each competition index at a time; β_1, …, β_7 refers to fixed parameters; i = 1, …, M are study sites; j = 1, …, n_i refers to a sample plot; α_i and c_{ij} are normally distributed random effects for study site *i* and sample plot *j* within study site *i*, respectively, with mean zero and an unknown, unrestricted variance–covariance matrix; and $\in_{ij}$ is a residual error with mean zero and unknown variance.

In Study **II**, first outliers—defined as values more than three times the interquartile range from the first and third quartiles of ΔV—were removed, resulting in the inclusion of 219 Scots pine, 112 Norway spruce, and 77 birch trees in the analysis. Then, the reliability of measurements derived from bi-temporal, multisensor point clouds was assessed by examining the consistency of tree attributes (e.g., stem volume and crown structure metrics) between T1 and T2. This was done using Pearson's correlation coefficient (*r*) and visual inspection with scatterplots to validate the use of the applied methodologies for observing changes in tree structures. The linear relationships between ΔV and crown structural metrics at T1, along with ΔC, were subsequently examined using *r* to gauge relationship strength. Statistical significance was assessed through *p*-values (*p*), with a 95% confidence level. These analyses were conducted across various tree species to identify growth dependencies unique to each species.

To further explore species-specific relationships between ΔV, crown structure, and ΔC, a random forest (RF) model was used. This approach enabled the exploration of potential non-linearities in the relationships, especially regarding the distribution of ΔV. Additionally, the RF model is ideal for handling complex predictor interactions and can mitigate collinearity to some extent, owing to its ensemble structure of decision trees (Breiman 2001). The full sample size was used to build the RF model to leverage all available data for identifying tree growth dependencies, ensuring that the model captured the complete variability present. To address collinearity among crown metrics, only the most strongly correlating crown metrics at T1 (with $r > 0.8$) were retained, while redundant ones were removed. This step minimized excessive correlation among predictors, reducing the risk of multicollinearity impacting model performance. The Gini index was then applied to calculate the relative importance of each selected predictor, quantifying the extent to which each metric contributes to reducing node impurity in the decision trees (Hapfelmeier et al. 2014). These importance values were scaled to a 0–100 range for easier comparison.

In Study **III**, *r* was utilized to assess the relationships between laser scanning-derived and *in situ*-based CIs. It was also used to evaluate which CI_{dbh}/CI_H or basal area increment had a stronger association with the laser scanning-based CIs. The consistency between the TLS-based and their corresponding ALS-based CIs was evaluated using *r*. In Study **III**, the potential difference between the laser scanning-derived CIs and *in situ*-based CIs was also analyzed, along with the effects of forest structural variability in the observed differences (ΔCIs). This was done to improve our knowledge of the performance of the implemented methodologies in boreal forest conditions. Hence, for the object-based CIs, the corresponding

ΔCIs were calculated by subtracting the *in situ*-based CI_{dbh} values from those based on laser scanning. For the point cloud-based CIs, the initial CI values were first normalized by dividing them by the maximum observed values. The ΔCIs were then calculated by subtracting the rescaled *in situ*-based CI_{dbh} values from the laser scanning-based CI values.

According to existing knowledge, increased tree density and complexity decrease the potential of current-generation laser scanning technology to detect all trees (Maltamo et al. 2004; Yrttimaa et al. 2019). The object-based and point cloud-based CIs implemented in this thesis must account for all vegetative structures around the target tree. Failure to include these structures may result in inaccurate CI predictions. Given these considerations, it can be assumed that as the number of surrounding trees in the field competing with the target tree increases, the uncertainty in laser scanning-based CI estimates will also rise. To investigate this, initially, the relationship between ΔCIs and the number of competitor trees, as identified through *in situ* measurements, was examined, using r to assess the strength of this relationship. Additionally, the relationship between the plot-level tree detection rate and tree density within the sample plots was explored to better understand how forest structure affects the ability of laser scanning point clouds to characterize tree competition. Accurate detection of trees is critical for reliable CI prediction, making it essential for assessing competitive stress. It is important to note that the relationships mentioned above were also evaluated for statistical significance using p-values.

3 RESULTS AND DISCUSSION

3.1 Influence of thinning treatments on stem and crown CIs derived from TLS (Study I)

The results of Study **I** showed that overall, as anticipated, competition levels were highest in the control plots (without thinning); see Figure 3. This aligns with studies by Baniya and Mandal (2018) and del Río et al. (2017) and can be explained by limited tree growth space. In addition, the results showed that competition magnitudes, as identified by CIs, were 12.8–52.7% smaller under moderate thinning treatments and 63.1–82.5% smaller under intensive thinning treatments compared to the control plots (no thinning). This declining trend was evident for both stem- and crown-based CIs (Figure 3). Moreover, intensive thinning from below, followed by intensive thinning from above, mainly led to a smaller mean and standard deviation compared to other thinning treatments of varying types and intensities (Figure 3). For moderate and intensive thinning from below, the magnitude of competition was 50.7% to 52.7% and 81.6% to 82.5%, respectively, smaller compared to the control plots when measured by CIs based on stem characteristics (CI_{dbh} and CI_H). In contrast, for moderate and intensive thinning from above, the magnitude of competition was 23% to 25% and 71.2% to 73.2%, respectively, smaller compared to the control plots when measured by CIs based on stem characteristics.

As mentioned above, most thinning treatments reduced competition, except systematic treatment and moderate-intensity thinning from above (Figure 3). These treatments produced a competition magnitude comparable to that of the control plots in terms of both mean and standard deviation. In general, more intensive thinning treatments resulted in greater reductions in competition as measured by the CIs compared to moderate thinning treatments.

As a result, we anticipate greater availability of growth resources, including space, nutrients, water, and sunlight, following intensive thinning treatments as they increase the space available for individual trees (Pretzsch 2009). In addition, thinning from below greatly reduced competition magnitude compared to thinning from above and systematic thinning (Figure 3). This can be attributed to the removal of smaller trees, which play a substantial role in taking up available growth resources, in the thinning from below treatment (Thorpe et al. 2010).

The findings from the nested two-level linear mixed-effects model provide quantitative insights into the differences in CIs across various thinning treatments and intensities. Moderate and intensive thinning from below, intensive thinning from above, and intensive systematic thinning all showed statistically significant differences from the control plots across all crown- and stem-based CIs ($p \leq 0.05$). However, only the stem-based CIs in moderate thinning from above differed significantly from control plots at the 95% confidence level. In contrast, there was no significant difference between control plots and moderate systematic thinning regarding all CIs ($p \geq 0.05$). There was also no statistically significant difference in competition between moderate thinning from above and systematic thinning treatments. This similarity could stem from both treatments' focus on removing larger individual trees (Saarinen et al. 2020). Although moderate-intensity systematic thinning created additional growing space for remaining trees, it did not significantly impact competition responses among individual Scots pine trees.

Through Study **I**, we found that TLS is an effective tool for quantifying competition by characterizing stem and crown structure in great detail. The ability to quantify both stem-based and crown-based CIs with TLS allowed us to distinguish subtle differences in tree competition under varying thinning treatments. However, it is important to note that the sample plots of this study are managed forest stands (the TLS tree detection rate was 98.8%), where structural characteristics are often influenced by silvicultural interventions and do not fully represent the complexity of unmanaged or natural forest ecosystems.

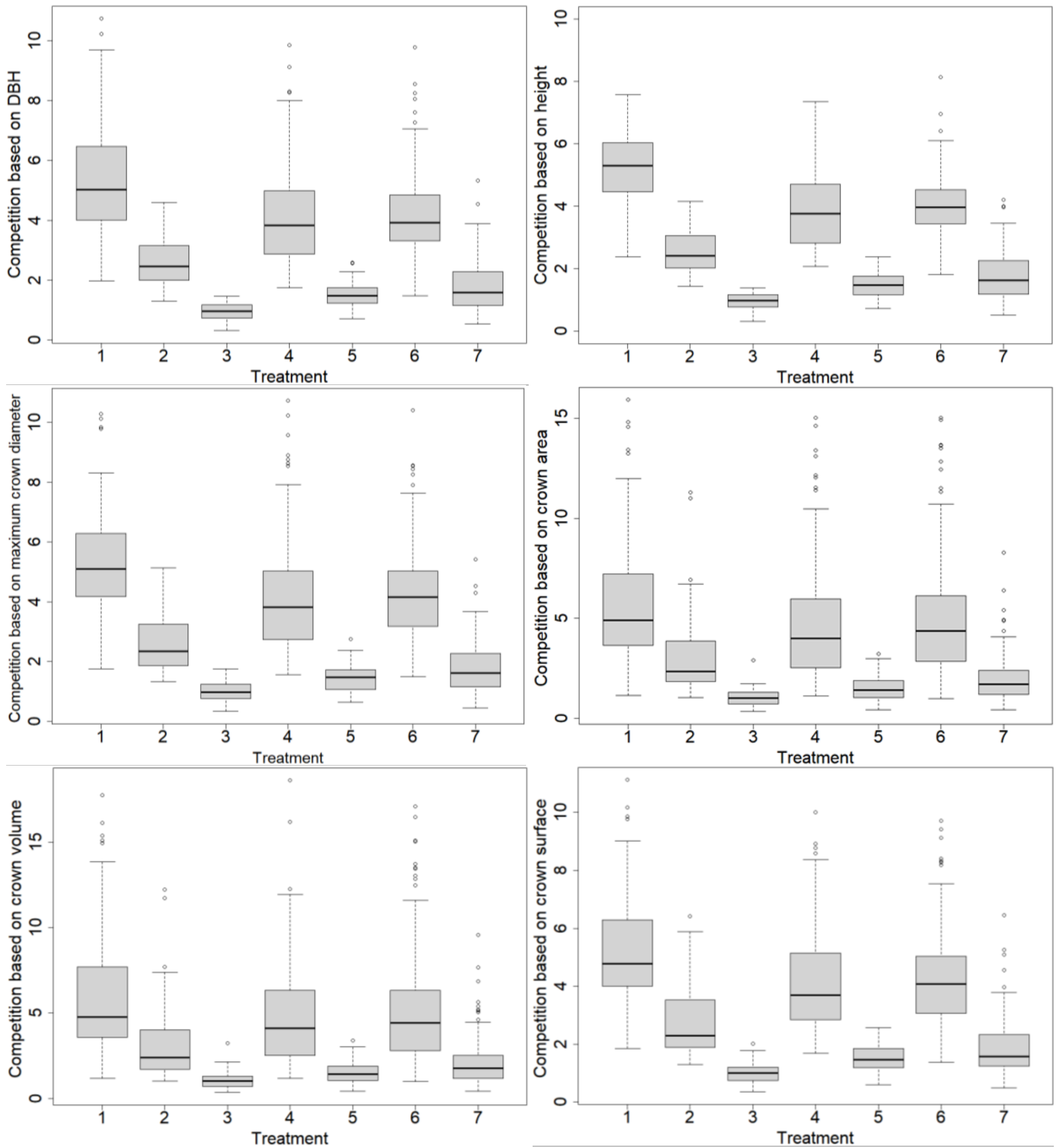

Figure 3. Variation in competition indices resulting from seven thinning treatments applied during 2005–2006. The treatments are as follows: 1 = control plots, 2 = moderate thinning from below, 3 = intensive thinning from below, 4 = moderate thinning from above, 5 = intensive thinning from above, 6 = moderate systematic thinning from above, and 7 = intensive systematic thinning from above.

3.2 Feasibility of using point clouds to detect crown metric increments and explain species-specific stem volume growth (Study II)

The assessment of consistency between individual tree characteristics measured at T1 and T2 showed that CH_{max} had the most consistent change over time ($r > 0.97$). In addition, CV showed an increasing trend over time, with correlations of 0.85 for Scots pine, 0.82 for Norway spruce, and 0.74 for birch trees, although there was a moderate degree of variability. Other crown metrics showed more variability around the 1:1 line. The least consistency was noted for CA_{3D}/CV in Scots pine, Norway spruce, and birch trees, with correlations of 0.65, 0.56, and 0.40, respectively.

The results also showed that both initial crown metrics and their changes had a significant relationship with ΔV, with explanatory power varying across different tree species, although it may reflect dynamics that differ from those observed over a longer period. Moreover, depending on internal tree characteristics and the stem itself, beyond the crown structure, growth allocation might vary (Pretzsch 2020), an aspect that was not addressed in our study. Other factors such as site conditions, tree age, mean tree size of the stand, and provenance could also influence the observed relationships (Pretzsch et al. 2022). Further research is required to explore how multisensor point clouds can contribute to understanding the growth distribution of various tree species.

Crown metrics at T1 demonstrated a stronger linear correlation with ΔV than metrics related to crown changes, which is consistent with the work of Yrttimaa et al. (2022b). This suggests that trees might initially expand their crowns, with larger crown sizes contributing to a higher ΔV. A strong relationship was observed between the ΔV of Scots pine and various crown metrics, such as CH_{max}, CA_{2D}, and CP. Additionally, the two 2D crown metrics, CA_{2D} and CP, demonstrated a significant correlation with the ΔV in birch. In contrast to pine trees, the volume change ΔV in Norway spruce showed the strongest correlations with 3D crown metrics, such as CA_{3D}, CV, and ΔCV.

By incorporating crown structural metrics and their ΔC into the RF model, we could explain 50%, 20%, and 6% of the variation in ΔV of Scots pine, Norway spruce, and birch, respectively (Figure 4). Based on the scaled mean decrease in the Gini index, CH_{max} was the most important metric for determining Scots pine ΔV, with CP and CA_{3D} also being important metrics. When predicting Norway spruce ΔV, ΔCV emerged as the most effective metric, followed by CV and ΔCA_{3D} as the second and third most influential metrics, respectively. For birch ΔV, ΔCV was identified as the primary predictor, with CP and CA_{3D} ranking as the next two most important metrics.

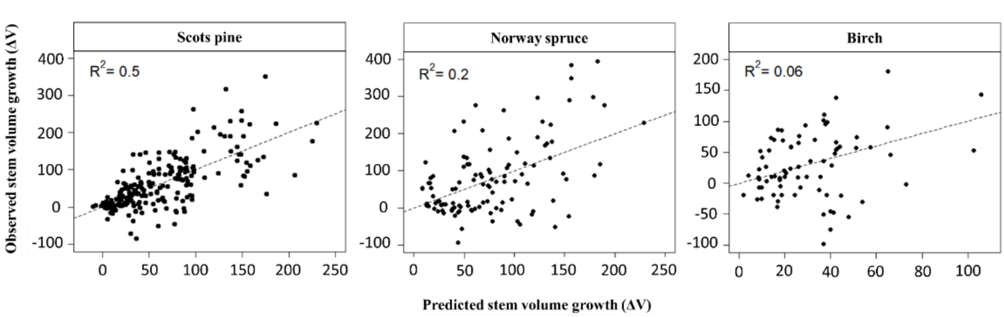

Figure 4. Scatter plot illustrating the relationship between observed and predicted stem volume growth (ΔV, in dm^3) for Scots pine, Norway spruce, and birch trees. The dashed line indicates the 1:1 relationship.

The similarity in key metrics for predicting ΔV of Norway spruce and birch indicates that both species continue to develop their crowns to sustain their growth rates. CH_{max} was also identified as one of the most important metrics for Norway spruces and birches, albeit with a lesser impact. This implies that trees with a higher CH_{max} may possess a competitive advantage, contributing to an increase in ΔV. In particular, the importance of CH_{max} in explaining the stem volume growth of Scots pine emphasizes the species' need for light, as it grows rapidly in height to optimize light acquisition (Givnish 1988). As seen above, CP was also an important metric for explaining the ΔV of Scots pine and birch. This can be attributed to the fact that a larger CP allows for greater light capture, which enhances photosynthetic activity and subsequently boosts the tree's growth, leading to an increase in ΔV (Poorter et al. 2012). The findings of this study must be interpreted with caution, as the relationships observed are inherently complex and may be influenced by a range of factors, such as stand density, site conditions, tree age, and mean tree size (Pretzsch et al. 2022). For example, Valentine et al. (2012) showed that higher stand density can limit crown expansion, with the reduced crown size potentially restricting the tree's ability to capture light and ultimately slowing its growth. Such complexities underscore the importance of considering these results in the broader context of forest dynamics and management practices.

3.3 Ability of TLS and ALS data to describe stem and crown competition (Study III)

The results of Study **III** showed that the effectiveness of laser scanning point clouds in reflecting individual trees' competitive status differed based on the competition index used, with correlations reaching up to 0.44 for TLS and 0.48 for ALS. However, object-based CIs were better correlated (r = 0.33 to 0.48) with *in situ*-based CIs than point cloud-based CIs (r = −0.22 to 0.37). This difference can arise from the distinct methodologies of the two CI types in characterizing competition compared to the *in situ*-based CIs. While object-based CIs were calculated using the Hegyi equation, similar to *in situ*-based CIs, with the main difference being the use of tree attributes derived from TLS and ALS point clouds as input data, point cloud-based CIs focused on assessing competitive stress by measuring the extent of vegetative structures within the target tree's estimated growing space, which was assumed to better characterize competition. Unlike point cloud-based CIs, neither object-based nor *in situ* CIs considered the shape of neighboring tree crowns or their shading impact, which may partly explain the varying correlations observed between point cloud-based and *in situ* CIs.

Regarding consistency between predicted TLS CIs and the corresponding ALS CIs, object-based CIs (r = 0.65 to 0.71, p < 0.001) were more consistent than point cloud-based CIs (r = 0.29 to 0.53, p < 0.001). Within the object-based CIs, CI_H exhibited the strongest correlation between TLS and ALS, while among the point cloud-based CIs, CDI showed the strongest correlation between TLS and ALS (r = 0.53), followed by $CI_{Cylinder}$ (r = 0.45, p < 0.001) and CPI (r = 0.29, p < 0.001). Inconsistency between the same CIs derived from TLS and ALS most likely originates from the distinct viewing angles and acquisition geometry of each system (Hilker et al. 2012; Kükenbrink et al. 2017). In other words, TLS produces a distinct point cloud reconstruction of trees compared to low-altitude ALS data. Consequently, it is reasonable to anticipate that point cloud-based CIs may vary depending on the type of point cloud data utilized. For example, the inconsistency between CPI_{TLS} and CPI_{ALS} can be attributed to varying occlusion effects caused by their distinct measurement geometries. In TLS, occlusion primarily affects the upper and middle parts of the tree crown (Béland et al. 2011, 2014)whereas ALS tends to capture treetops with less occlusion but may overlook lower canopy layers, especially in dense canopies (Kükenbrink et al. 2017).

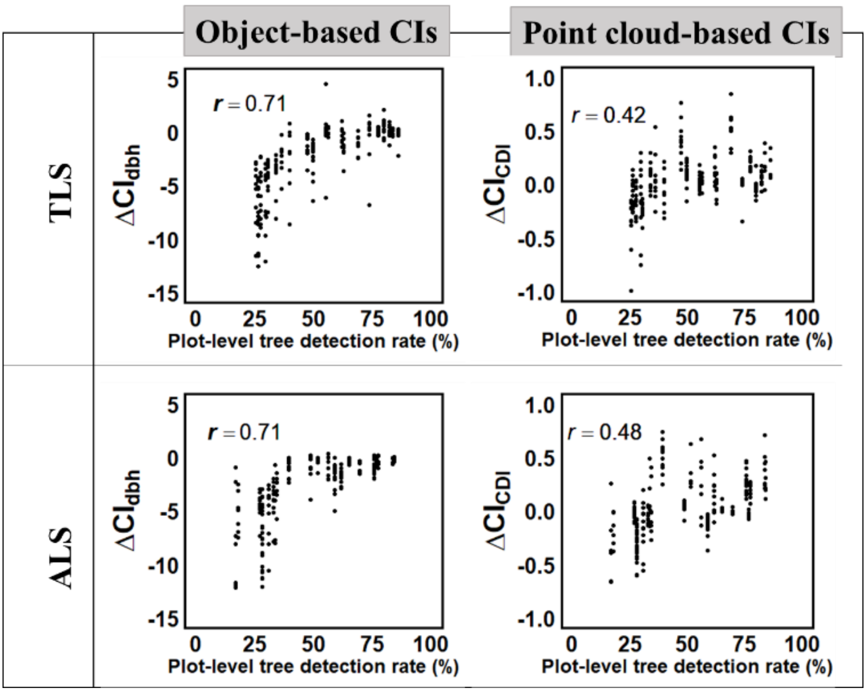

Figure 5. An example of the relationship between plot-level tree detection rate and difference (Δ) in competition indices (CIs) derived from terrestrial laser scanning (TLS) and airborne laser scanning (ALS) in comparison to *in situ* data. The analyzed CIs were based on diameter at breast height (CI_{dbh}) and canopy density index (CDI).

Based on the results, as the number of neighboring trees increased and the tree detection rate decreased, the difference between laser scanning-based CIs and *in situ*-based CIs (ΔCIs) increased (Figure 5). Overall, object-based CIs were more influenced (r = 0.68 to 0.84, p < 0.001) by detection rate than point cloud-based CIs (r = 0.25 to 0.49, p < 0.001). The number of neighboring trees in the field representing the complexity of the forest structure had a negative effect on the accuracy of estimations, especially for object-based CIs (r = −0.79 to −0.96, p < 0.001). In this study, both TLS and ALS tended to underestimate trees' competitive status relative to *in situ*-based CIs, primarily because they could not detect all competitive neighboring trees surrounding the target trees. In practice, the tree detection rate is linked to the complexity of the forest structure, often due to the omission of intermediate and suppressed trees (Wang et al. 2016). Vauhkonen et al. (2012) reported that forest structure significantly impacts detection accuracy, with complex structures negatively affecting detection rates. In this study, neither TLS nor ALS could detect all trees, leading to an underestimation of the resulting competitive stress. Figure 5 illustrates an example of the relationship between the plot-level tree detection rate and ΔCIs, comparing both TLS- and ALS-based object-based and point cloud-based CIs.

3.4 Constraints and future research

In Study **I**, we aimed to develop approaches for assessing stem and crown competition using TLS data to evaluate the effects of different types and intensities of thinning treatments on stem- and crown-based CIs in Scots pine stands. Although this study yielded promising results in describing stem- and crown-based competition between trees, further research is needed due to its limitations. The scanning setup, tree delineation, and segmentation algorithms could create uncertainties, such as point cloud occlusion and inaccurate delineation of tree crowns, in this study. However, advances in laser scanning technologies such as TLS, ALS, and multisensor approaches, along with methodological improvements (e.g., in crown segmentation algorithms), are expected to enhance the accuracy of results in similar studies in the future. With the availability of time series of laser scanning point cloud data, monitoring the impact of thinning treatments on competition between trees, especially by employing point cloud-based CIs, is recommended for future research.

The objective of Study **II** was to understand the dependencies between individual tree stem volume growth (ΔV) and crown structure, including its change (ΔC), using TLS and ALS point clouds. This study revealed some negative ΔV values, likely due to inaccurate taper curve estimation due to point cloud occlusion. The co-registration accuracy between the terrestrial and aerial point clouds and the discrepancy in the methods used at T1 and T2 are also sources of uncertainty that may have affected the results. These uncertainties could have led to a spatial mismatch between the trees identified at T1 and T2, which could have decreased the reliability of the tree-to-tree matching. In addition, our data in Study **II** were mostly collected during leaf-off conditions, likely resulting in an underestimation of the crown characteristics of the birch trees. Incorporating partial dependency plots or using Generalized Additive Models could enhance the interpretability of the results. For future studies, a deeper investigation into the role of multisensor point clouds in analyzing growth allocation patterns for different tree species is recommended. One possibility can be focusing on understanding appropriate time intervals to filter out excessive noise and reveal genuine patterns in forest change detection, especially in slow-growth boreal forests.

In Study **III,** we investigated the capacity of TLS and ALS data to characterize competitive stress affecting individual trees. Based on the results of this study, the predicted competition through laser scanning data was subject to underestimation compared to *in situ*-based competition. The primary reason for this underestimation is that the laser scanning systems used in this study could not capture all the competitive neighbor trees surrounding the target trees, especially in complex forest stands. Hence, point cloud occlusion was an uncertainty source. This limitation can be addressed in future studies through careful planning of the data acquisition campaign, with a focus on obtaining a comprehensive point cloud reconstruction of all individual trees and capturing the full extent of vegetative structures within the competitive neighborhood of the target trees. One alternative approach to overcoming the challenge of point cloud occlusion is the fusion of terrestrial and aerial point clouds, as each system offers different viewpoints. Automatic segmentation of point clouds often faces issues such as data omissions and the inaccurate delineation of tree crowns in aerial point clouds or stems in terrestrial point clouds (Kwak et al. 2007), which can lead to errors in the prediction of object-based CIs. Thus, methodological improvements are needed to enhance tree characterization for more accurate competition assessments. Since the laser scanning datasets for Studies **II** and **III** are identical, the limitations and recommendations outlined for Study **III** are largely applicable to Study **II** as well.

4 CONCLUSIONS

In recent decades, laser scanning has become an increasingly important tool in forest mapping due to its capability to provide highly detailed 3D information on trees and forest stands. This thesis emphasizes the feasibility of using laser scanning point clouds to understand forest dynamics, particularly in the context of competition, tree growth, and forest management strategies in boreal forests.

Study **I** highlighted the utility of TLS technology in deriving both stem and crown metrics, allowing for a more comprehensive assessment of how different thinning treatments affect competition between trees at both stem and crown levels. This approach increased our understanding of how thinning influences tree growth dynamics. In addition, this study demonstrated the impact of various thinning treatments on TLS-derived stem and crown CIs, offering insights for optimizing forest management practices. For example, it showed that intensive thinning from below significantly reduced competition by up to 82.5% compared with other treatments. In contrast, moderate thinning treatments showed limited effects, underscoring the need for management strategies. This study also emphasized the importance of TLS point clouds in characterizing crown metrics for competition assessments, which are often overlooked in traditional methods.

Study **II** underscored the potential of bi-temporal, multisensor point clouds from TLS and ALS in linking crown structural changes to stem volume growth across three important species in boreal forests. The results of Study **II** revealed species-specific variations in how crown metrics and their changes influence growth, with Scots pine showing the strongest correlations (explaining 50% of ΔV), while Norway spruce and birch trees had a ΔV of 20% and 6%, respectively. In addition, we found that crown structural metrics at T1 exhibited a stronger correlation with species-specific ΔV compared to ΔC-related metrics at a 95% confidence interval. The study highlighted the potential of detailed point cloud data in monitoring tree growth and inventorying forests on larger scales, although operational challenges, such as the cost of data collection, remain significant barriers to large-scale application.

Study **III** confirmed the ability of TLS and low-altitude ALS point clouds to effectively quantify the competitive stress of individual trees. However, it also identified challenges, such as point cloud occlusion and the subsequent non-detection of all relevant neighboring trees, including both individual trees and vegetative structures. Overall, the competition effects described using low-altitude ALS and TLS data were very similar. This finding opens pathways for integrating competition assessments into operational forest management workflows, such as determining thinning priorities.

Together, the findings of these three studies underscore the value of laser scanning technologies in advancing forest ecology research and informing sustainable forest management practices. By bridging gaps in competition assessment, growth prediction, and large-scale inventory methods, this research provides valuable insights for developing sustainable forest management strategies, particularly in the boreal context. Future advancements in sensor technology and data affordability could further enhance the practical applications of these methodologies.

REFERENCES

Baniya B, Mandal RA (2018) Assessment of Plant Competition and Tree Typical Crown Area in Thinned and Unthinned Stands of Community Managed Pine Plantation. Ann Archaeol 1: 42–47

Béland M, Widlowski J-L, Fournier RA, Côté J-F, Verstraete MM (2011) Estimating leaf area distribution in savanna trees from terrestrial LiDAR measurements. Agric For Meteorol 151: 1252–1266. https://doi.org/10.1016/j.agrformet.2011.05.004

Béland M, Baldocchi DD, Widlowski J-L, Fournier RA, Verstraete MM (2014) On seeing the wood from the leaves and the role of voxel size in determining leaf area distribution of forests with terrestrial LiDAR. Agric For Meteorol 184: 82–97. https://doi.org/10.1016/j.agrformet.2013.09.005

Bollandsås OM, Næsset E (2009) Weibull models for single-tree increment of Norway spruce, Scots pine, birch and other broadleaves in Norway. Scand J For Res 24: 54–66. https://doi.org/10.1080/02827580802477875

Breiman L (2001) Random forests. Mach Learn 45: 5–32. https://doi.org/10.1023/A:1010933404324/METRICS

Burkhart HE, Tomé M (2012) Modeling forest trees and stands. Model For Trees Stands 9789048131: 1–457. https://doi.org/10.1007/978-90-481-3170-9

Calders K, Adams J, Armston J, Bartholomeus H, Bauwens S, Bentley LP, Chave J, Danson FM, Demol M, Disney M, Gaulton R, Krishna Moorthy SM, Levick SR, Saarinen N, Schaaf C, Stovall A, Terryn L, Wilkes P, Verbeeck H (2020) Terrestrial laser scanning in forest ecology: Expanding the horizon. Remote Sens Environ 251: 112102. https://doi.org/10.1016/j.rse.2020.112102

Contreras MA, Affleck D, Chung W (2011) Evaluating tree competition indices as predictors of basal area increment in western Montana forests. For Ecol Manage 262: 1939–1949. https://doi.org/10.1016/j.foreco.2011.08.031

Dassot M, Constant T, Fournier M (2011) The use of terrestrial LiDAR technology in forest science: Application fields, benefits and challenges. Ann For Sci 68: 959–974.

https://doi.org/10.1007/s13595-011-0102-2

Del Río M, Bravo-Oviedo A, Pretzsch H, Löf M, Ruiz-Peinado R (2017) A review of thinning effects on Scots pine stands: From growth and yield to new challenges under global change. For Syst 26: eR03S. https://doi.org/10.5424/fs/2017262-11325

Fassnacht FE, White JC, Wulder MA, Næsset E (2024) Remote sensing in forestry: current challenges, considerations and directions. For An Int J For Res 97: 11–37. https://doi.org/10.1093/forestry/cpad024

Givnish T (1988) Adaptation to Sun and Shade: a Whole-Plant Perspective. Funct Plant Biol 15: 63. https://doi.org/10.1071/PP9880063

Hapfelmeier A, Hothorn T, Ulm K, Strobl C (2014) A new variable importance measure for random forests with missing data. Stat Comput 24: 21–34. https://doi.org/10.1007/s11222-012-9349-1

Hegyi F (1974) A simulation model for managing jack-pine stands. Growth Model tree stand Simul 74–90

Hilker T, Coops NC, Newnham GJ, van Leeuwen M, Wulder MA, Stewart J, Culvenor DS (2012) Comparison of Terrestrial and Airborne LiDAR in Describing Stand Structure of a Thinned Lodgepole Pine Forest. J For 110: 97–104. https://doi.org/10.5849/jof.11-003

Holopainen M, Vastaranta M, Kankare V, Räty M, Vaaja M, Liang X, Yu X, Hyyppä J, Hyyppä H, Viitala R, Kaasalainen S (2012) BIOMASS ESTIMATION OF INDIVIDUAL TREES USING STEM AND CROWN DIAMETER TLS MEASUREMENTS. Int Arch Photogramm Remote Sens Spat Inf Sci XXXVIII-5/: 91–95. https://doi.org/10.5194/isprsarchives-XXXVIII-5-W12-91-2011

Isenburg M (2019) LAStools—Efficient LiDAR Processing Software,(version 181001 academic); rapidlasso GmbH: Gilching, Germany

Kaasalainen S, Krooks A, Liski J, Raumonen P, Kaartinen H, Kaasalainen M, Puttonen E, Anttila K, Mäkipää R (2014) Change Detection of Tree Biomass with Terrestrial Laser Scanning and Quantitative Structure Modelling. Remote Sens 6: 3906–3922. https://doi.org/10.3390/rs6053906

Kalliovirta J, Tokola T (2005) Functions for estimating stem diameter and tree age using tree height, crown width and existing stand database information. Silva Fenn 39: 227–248

Khosravipour A, Skidmore AK, Isenburg M (2016) Generating spike-free digital surface models using LiDAR raw point clouds: A new approach for forestry applications. Int J Appl Earth Obs Geoinf 52: 104–114. https://doi.org/10.1016/j.jag.2016.06.005

Kükenbrink D, Schneider FD, Leiterer R, Schaepman ME, Morsdorf F (2017) Quantification of hidden canopy volume of airborne laser scanning data using a voxel traversal algorithm. Remote Sens Environ 194: 424–436. https://doi.org/10.1016/j.rse.2016.10.023

Kwak D-A, Lee W-K, Lee J-H, Biging GS, Gong P (2007) Detection of individual trees and estimation of tree height using LiDAR data. J For Res 12: 425–434. https://doi.org/10.1007/s10310-007-0041-9

LaRue EA, Hardiman BS, Elliott JM, Fei S (2019) Structural diversity as a predictor of ecosystem function. Environ Res Lett 14: 114011. https://doi.org/10.1088/1748-9326/ab49bb

Latham PA, Zuuring HR, Coble DW (1998) A method for quantifying vertical forest structure. For Ecol Manage 104: 157–170

Lefsky MA, McHale MR (2008) Volume estimates of trees with complex architecture from terrestrial laser scanning. J Appl Remote Sens 2: 023521.

https://doi.org/10.1117/1.2939008
Liang X, Kankare V, Hyyppä J, Wang Y, Kukko A, Haggrén H, Yu X, Kaartinen H, Jaakkola A, Guan F, Holopainen M, Vastaranta M (2016) Terrestrial laser scanning in forest inventories. ISPRS J Photogramm Remote Sens 115: 63–77. https://doi.org/10.1016/j.isprsjprs.2016.01.006
Liang X, Hyyppä J, Kaartinen H, Lehtomäki M, Pyörälä J, Pfeifer N, Holopainen M, Brolly G, Francesco P, Hackenberg J, Huang H, Jo HW, Katoh M, Liu L, Mokroš M, Morel J, Olofsson K, Poveda-Lopez J, Trochta J, Wang D, Wang J, Xi Z, Yang B, Zheng G, Kankare V, Luoma V, Yu X, Chen L, Vastaranta M, Saarinen N, Wang Y (2018) International benchmarking of terrestrial laser scanning approaches for forest inventories. ISPRS J Photogramm Remote Sens 144: 137–179. https://doi.org/10.1016/j.isprsjprs.2018.06.021
Ma Q, Su Y, Tao S, Guo Q (2018) Quantifying individual tree growth and tree competition using bi-temporal airborne laser scanning data: a case study in the Sierra Nevada Mountains, California. Int J Digit Earth 11: 485–503. https://doi.org/10.1080/17538947.2017.1336578
Maas H -G., Bienert A, Scheller S, Keane E (2008) Automatic forest inventory parameter determination from terrestrial laser scanner data. Int J Remote Sens 29: 1579–1593. https://doi.org/10.1080/01431160701736406
Maltamo M, Mustonen K, Hyyppä J, Pitkänen J, Yu X (2004) The accuracy of estimating individual tree variables with airborne laser scanning in a boreal nature reserve. Can J For Res 34: 1791–1801. https://doi.org/10.1139/x04-055
Maltamo M, Næsset E, Vauhkonen J (2014) Forestry applications of airborne laser scanning. Concepts case Stud Manag Ecosys 27: 460
Mehtätalo L, Lappi J (2020) Biometry for Forestry and Environmental Data. Chapman and Hall/CRC, Boca Raton, FL : CRC Press, 2020. | Series: Chapman & Hall/CRC applied environmental statistics
Metz J, Seidel D, Schall P, Scheffer D, Schulze E-D, Ammer C (2013) Crown modeling by terrestrial laser scanning as an approach to assess the effect of aboveground intra- and interspecific competition on tree growth. For Ecol Manage 310: 275–288. https://doi.org/10.1016/j.foreco.2013.08.014
Meyer F, Beucher S (1990) Morphological segmentation. J Vis Commun Image Represent 1: 21–46. https://doi.org/10.1016/1047-3203(90)90014-M
Muhojoki J, Tavi D, Hyyppä E, Lehtomäki M, Faitli T, Kaartinen H, Kukko A, Hakala T, Hyyppä J (2024) Benchmarking Under- and Above-Canopy Laser Scanning Solutions for Deriving Stem Curve and Volume in Easy and Difficult Boreal Forest Conditions. Remote Sens 16: 1721. https://doi.org/10.3390/rs16101721
Newnham GJ, Armston JD, Calders K, Disney MI, Lovell JL, Schaaf CB, Strahler AH, Danson FM (2015) Terrestrial Laser Scanning for Plot-Scale Forest Measurement. Curr For Reports 1: 239–251. https://doi.org/10.1007/s40725-015-0025-5
Olivier M-D, Robert S, Fournier RA (2016) Response of sugar maple (Acer saccharum, Marsh.) tree crown structure to competition in pure versus mixed stands. For Ecol Manage 374: 20–32. https://doi.org/10.1016/j.foreco.2016.04.047
Pedersen RØ, Bollandsås OM, Gobakken T, Næsset E (2012) Deriving individual tree competition indices from airborne laser scanning. For Ecol Manage 280: 150–165. https://doi.org/10.1016/j.foreco.2012.05.043
Pedersen RØ, Næsset E, Gobakken T, Bollandsås OM (2013) On the evaluation of competition indices - The problem of overlapping samples. For Ecol Manage 310: 120–

133. https://doi.org/10.1016/j.foreco.2013.07.040
Pinheiro J, Bates D, DebRoy S, Sarkar D (2014) R Core Team (2014) nlme: linear and nonlinear mixed effects models. R package version 3.1-117
Pitkänen TP, Bianchi S, Kangas A (2022) Quantifying the effects of competition on the dimensions of Scots pine and Norway spruce crowns. Int J Appl Earth Obs Geoinf 112: 102941. https://doi.org/10.1016/j.jag.2022.102941
Pont D, Dungey HS, Suontama M, Stovold GT (2021) Spatial Models With Inter-Tree Competition From Airborne Laser Scanning Improve Estimates of Genetic Variance. Front Plant Sci 11. https://doi.org/10.3389/fpls.2020.596315
Poorter L, Lianes E, Moreno-de las Heras M, Zavala MA (2012) Architecture of Iberian canopy tree species in relation to wood density, shade tolerance and climate. Plant Ecol 213: 707–722. https://doi.org/10.1007/s11258-012-0032-6
Pretzsch H (2009) Growing Space and Competitive Situation of Individual Trees. In: Forest Dynamics, Growth and Yield. Springer Berlin Heidelberg, Berlin, Heidelberg, pp 291–336
Pretzsch H (2020) The course of tree growth. Theory and reality. For Ecol Manage 478: 118508. https://doi.org/10.1016/j.foreco.2020.118508
Pretzsch H, Ahmed S, Jacobs M, Schmied G, Hilmers T (2022) Linking crown structure with tree ring pattern: methodological considerations and proof of concept. Trees 36: 1349–1367. https://doi.org/10.1007/s00468-022-02297-x
Pyörälä J, Saarinen N, Kankare V, Coops NC, Liang X, Wang Y, Holopainen M, Hyyppä J, Vastaranta M (2019) Variability of wood properties using airborne and terrestrial laser scanning. Remote Sens Environ 235: 111474. https://doi.org/10.1016/j.rse.2019.111474
Roussel JR, Auty D (2018) LidR: Airborne LiDAR data manipulation and visualization for forestry applications. R CRAN Proj 1: 1
Saarinen N, Kankare V, Yrttimaa T, Viljanen N, Honkavaara E, Holopainen M, Hyyppä J, Huuskonen S, Hynynen J, Vastaranta M (2020) Assessing the effects of thinning on stem growth allocation of individual Scots pine trees. For Ecol Manage 474: 118344. https://doi.org/10.1016/j.foreco.2020.118344
Seidel D, Hoffmann N, Ehbrecht M, Juchheim J, Ammer C (2015) How neighborhood affects tree diameter increment – New insights from terrestrial laser scanning and some methodical considerations. For Ecol Manage 336: 119–128. https://doi.org/10.1016/j.foreco.2014.10.020
Su Y, Guo Q, Fry DL, Collins BM, Kelly M, Flanagan JP, Battles JJ (2016) A Vegetation Mapping Strategy for Conifer Forests by Combining Airborne LiDAR Data and Aerial Imagery. Can J Remote Sens 42: 1–15. https://doi.org/10.1080/07038992.2016.1131114
Tempel DJ, Gutiérrez RJ, Battles JJ, Fry DL, Su Y, Guo Q, Reetz MJ, Whitmore SA, Jones GM, Collins BM, Stephens SL, Kelly M, Berigan WJ, Peery MZ (2015) Evaluating short- and long-term impacts of fuels treatments and simulated wildfire on an old-forest species. Ecosphere 6. https://doi.org/10.1890/ES15-00234.1
Terryn L, Calders K, Bartholomeus H, Bartolo RE, Brede B, D'hont B, Disney M, Herold M, Lau A, Shenkin A, Whiteside TG, Wilkes P, Verbeeck H (2022) Quantifying tropical forest structure through terrestrial and UAV laser scanning fusion in Australian rainforests. Remote Sens Environ 271: 112912. https://doi.org/10.1016/j.rse.2022.112912
Thorpe HC, Astrup R, Trowbridge A, Coates KD (2010) Competition and tree crowns: A

neighborhood analysis of three boreal tree species. For Ecol Manage 259: 1586–1596. https://doi.org/10.1016/j.foreco.2010.01.035

Tomé M, Burkhart HE (1989) Distance-Dependent Competition Measures for Predicting Growth of Individual Trees. For Sci 35: 816–831. https://doi.org/10.1093/forestscience/35.3.816

Tompalski P, Coops N, White J, Wulder M (2016) Enhancing Forest Growth and Yield Predictions with Airborne Laser Scanning Data: Increasing Spatial Detail and Optimizing Yield Curve Selection through Template Matching. Forests 7: 255. https://doi.org/10.3390/f7110255

Twery MJ, Weiskittel AR (2013) Forest-Management Modelling. In: Environmental Modelling. Wiley, pp 379–398

Valentine HT, Mäkelä A, Green EJ, Amateis RL, Mäkinen H, Ducey MJ (2012) Models relating stem growth to crown length dynamics: Application to loblolly pine and Norway spruce. Trees - Struct Funct 26: 469–478. https://doi.org/10.1007/s00468-011-0608-0

Vauhkonen J, Ene L, Gupta S, Heinzel J, Holmgren J, Pitkanen J, Solberg S, Wang Y, Weinacker H, Hauglin KM, Lien V, Packalen P, Gobakken T, Koch B, Naesset E, Tokola T, Maltamo M (2012) Comparative testing of single-tree detection algorithms under different types of forest. Forestry 85: 27–40. https://doi.org/10.1093/forestry/cpr051

Vauhkonen J, Maltamo M, McRoberts RE, Næsset E (2014) Introduction to Forestry Applications of Airborne Laser Scanning. 1–16. https://doi.org/10.1007/978-94-017-8663-8_1

Versace, Gianelle, Frizzera, Tognetti, Garfì, Dalponte (2019) Prediction of Competition Indices in a Norway Spruce and Silver Fir-Dominated Forest Using Lidar Data. Remote Sens 11: 2734. https://doi.org/10.3390/rs11232734

Wang Y, Hyyppa J, Liang X, Kaartinen H, Yu X, Lindberg E, Holmgren J, Qin Y, Mallet C, Ferraz A, Torabzadeh H, Morsdorf F, Zhu L, Liu J, Alho P (2016) International Benchmarking of the Individual Tree Detection Methods for Modeling 3-D Canopy Structure for Silviculture and Forest Ecology Using Airborne Laser Scanning. IEEE Trans Geosci Remote Sens 54: 5011–5027. https://doi.org/10.1109/TGRS.2016.2543225

Weiskittel AR, Hann DW, Kershaw JA, Vanclay JK (2011) Forest Growth and Yield Modeling. For Growth Yield Model. https://doi.org/10.1002/9781119998518

Wulder MA, Franklin SE (2003) Remote Sensing of Forest Environments, Introduction. The transition from theory to information. Remote Sens For Environ 3–12

Yrttimaa T, Saarinen N, Kankare V, Liang X, Hyyppä J, Holopainen M, Vastaranta M (2019) Investigating the Feasibility of Multi-Scan Terrestrial Laser Scanning to Characterize Tree Communities in Southern Boreal Forests. Remote Sens 11: 1423. https://doi.org/10.3390/rs11121423

Yrttimaa T, Saarinen N, Kankare V, Hynynen J, Huuskonen S, Holopainen M, Hyyppä J, Vastaranta M (2020) Performance of terrestrial laser scanning to characterize managed Scots pine (Pinus sylvestris L.) stands is dependent on forest structural variation. ISPRS J Photogramm Remote Sens 168: 277–287. https://doi.org/10.1016/j.isprsjprs.2020.08.017

Yrttimaa T, Luoma V, Saarinen N, Kankare V, Junttila S, Holopainen M, Hyyppä J, Vastaranta M (2022a) Exploring tree growth allometry using two-date terrestrial laser scanning. For Ecol Manage 518. https://doi.org/10.1016/j.foreco.2022.120303

Yrttimaa T, Luoma V, Saarinen N, Kankare V, Junttila S, Holopainen M, Hyyppä J, Vastaranta M (2022b) Monitoring Tree Growth Allometry Using Two-Date Terrestrial Laser Scanning. SSRN Electron J. https://doi.org/10.2139/ssrn.4021680

Zhou M, Lei X, Lu J, Gao W, Zhang H (2022) Comparisons of competitor selection approaches for spatially explicit competition indices of natural spruce-fir-broadleaf mixed forests. Eur J For Res 141: 177–211. https://doi.org/10.1007/s10342-021-01430-8

Zhu Z, Kleinn C, Nölke N (2021) Assessing tree crown volume—a review. For An Int J For Res 94: 18–35. https://doi.org/10.1093/forestry/cpaa037